Acta Astronautica 165 (2019) 219–228

Contents lists available at ScienceDirect

Acta Astronautica

journal homepage: www.elsevier.com/locate/actaastro

Enhanced GEANT4 Monte Carlo simulations of the space radiation effects on the International Space Station and Apollo missions using high-performance computing environment☆

Matthew Lund[a,*], Tatjana Jevremovic[b]

[a] 50 S. Central Campus Dr., Rm 1206, University of Utah, Nuclear Engineering Program, Salt Lake City, UT 84112, USA
[b] Water Reactor Technology Development, IAEA, Vienna, Austria

ARTICLE INFO

Keywords:
GEANT4
Space radiation environment
International Space Stations (ISS)
Apollo missions
Radiation dose

ABSTRACT

A significant challenge to current and future manned and/or unmanned space missions is due to deep space radiation. An improvement in more realistic (more accurate) simulation models in predicting the effects of radiation within the spacecraft is required, especially to better predict dose to astronauts, energy deposition within sensitive electronics, and effectiveness of radiation shielding for long-term space missions. The International Space Station provides an invaluable resource for long-term measurements of the radiation environment in Low Earth Orbit (LEO); however, the only manned missions with dosimetry data available beyond LEO are the Apollo missions. Thus the physiological effects and dosimetry for deep space missions are not well understood in planning extended missions. GEANT4, a Monte Carlo method, represents a powerful physics simulation tool to assess the effects of radiation transport through spacecraft. The newest version of GEANT4 supports multithreading and Message Passing Interface (MPI) allowing for much faster distributive processing of simulations, using a high-performance computing environment. This paper introduces a new simulation model and application using GEANT4 that greatly reduces computational time to hours instead of weeks without any post simulation processing based on high-performance computing. This paper also introduces a new set of GEANT4 computational detectors for calculating dose distribution, besides the historically used International Commission of Radiation Units simulation spheres. The computational detectors include a thermoluminescent detector, tissue equivalent proportional counter, and human phantom, along with additional new scorers to calculate dose equivalence based on the International Commission of Radiation Protection standards. This study presents GEANT4 simulations of the dose deposition for the International Space Station and the Apollo 11 and 14 missions, which replicate well the dose measurements during these missions. The simulations of both Apollo missions show consistent doses from galactic cosmic rays and radiation belts with a small variation in dose distribution across the Apollo capsule. The greatest contributor to radiation dose for both Apollo missions in the simulations came from galactic cosmic rays. Simulations of historical solar particle events during an Apollo missions show a solar particle event would not be fatal and below mission limits. These GEANT4 models also provides the values of the dose deposition and dose equivalent for various organs within a human phantom in the International Space Station and Apollo command module, which are developed for the first time using this GEANT4 based application.

1. Introduction

As astronauts and spacecrafts move further away from the Earth's protective atmosphere and magnetic field, the radiation dose increases due to solar particle events (SPE), galactic cosmic rays (GCR), and the trapped radiation belts. Charged heavy-Z ions with energies of 1 MeV to 1 TeV dominate the radiation environment [1]. These high energy particles easily pass through spacecraft and are very difficult to adequately shield without a large mass of shielding materials in the spacecraft. This increased radiation dose poses a serious health hazard to astronauts during long-duration or deep space missions, which may increase life-long cancer risk and other health effects to the astronauts.

☆ 66th International Astronautical Congress, Jerusalem, Israel. IAC-15-E5.1.5.

* Corresponding author.
E-mail address: matthewl.lund@utah.edu (M. Lund).

https://doi.org/10.1016/j.actaastro.2019.09.018
Received 6 January 2019; Received in revised form 20 June 2019; Accepted 15 September 2019
Available online 19 September 2019

Predicting the radiation dose during long-duration missions requires accurate numerical models of radiation transport capable of capturing all details of the geometry and flight, including more precise accounting of radiation interactions and energy deposition. The models also require accurate modeling of the human body for as accurate as possible dose predictions. Predicting the energy deposition within sensitive electronics is equally essential. Lastly, such comprehensive numerical models should easily model existing and new radiation shielding materials for future missions. The National Aeronautics and Space Administration (NASA) and international partners have made detailed long-term measurements of the radiation environment in low earth orbit (LEO) onboard the space shuttle and International Space Station (ISS), providing detail characterization of the environment [2]; however, only the manned Apollo missions to the Moon have dosimetry data collected beyond LEO. Historical data shows the Apollo 11 astronauts receiving a skin dose of 1.8 mGy; whereas, the data shows astronauts in Apollo 14 mission receiving a skin dose of 11.4 mGy, which is an order of magnitude greater dose compared to all other Apollo missions [3]. The cause of this difference in dose rate is still not well understood.

NASA has developed HZETRN [4] and OLTARIS [5], deterministic codes, whereas the European Space Agency (ESA) has developed MULASSIS [6] and GRAS [7] based on GEometry ANd Tracking 4 (GEANT4) to model and transport radiation in the space environment. Each simulation code is an independent computer software package that uses an input geometry file and particle spectrum file to simulate the radiation transport through a spacecraft and score radiation interactions. Previous applications in space radiation transport are single thread codes running a single calculation at a time. GEANT4 is a C++ toolkit, using the Monte Carlo method for simulating radiation transport of different types and energies through various geometries and environments [8]. The Monte Carlo method is a non-deterministic method used for solving radiation transport by randomly sampling, using a random number generator, a large number of particles and physics interactions to create a probability distribution. In this method, GEANT4 transports each particle through a volume step by step based on the step length determined by the cross-section of the physics processes selected. The newest version of GEANT4 supports multithreading [9] and Message Passing Interface (MPI) allowing for much faster distributive simulations across large high-performance computing cluster through massive parallelism with multiple simultaneous computations, reducing computational times from many weeks to just a few hours. GRAS and SPENVIS are tied to older single thread versions of GEANT4 not allowing for parallelism.

This paper presents a new simulation model and application based on the GEANT4 C++ toolkit developed to run in parallel, using the University of Utah Center for High-Performance Computing [10]. This model and application were used to model radiation dose on the ISS and during the Apollo missions quickly and precisely while accounting for as many known details in describing the space radiation environment. This new simulation model makes possible a precise prediction of astronaut dose and quick prototyping of new shielding designs.

2. Development of GEANT4 application and simulation model

In order to model radiation transport and interactions through a spacecraft, the numerical simulation modeling should ideally allow for easily varying spacecraft geometry, space radiation spectrum, particle generation, particle transport with correct physics processes, scoring of energy and dose deposition, normalization of the scored values, and analysis of error. Fig. 1 shows the simulation modeling steps required to model the space radiation environment through a spacecraft. To allow for varying geometries, the application in this model uses Geometry Description Markup Language (GDML) [11], which is an extension of XML language using tags to describe various components. The GEANT4 GDML parser reads and writes GDML files, which can also be read from the CERN ROOT analysis package. GDML supports GEANT4 solid

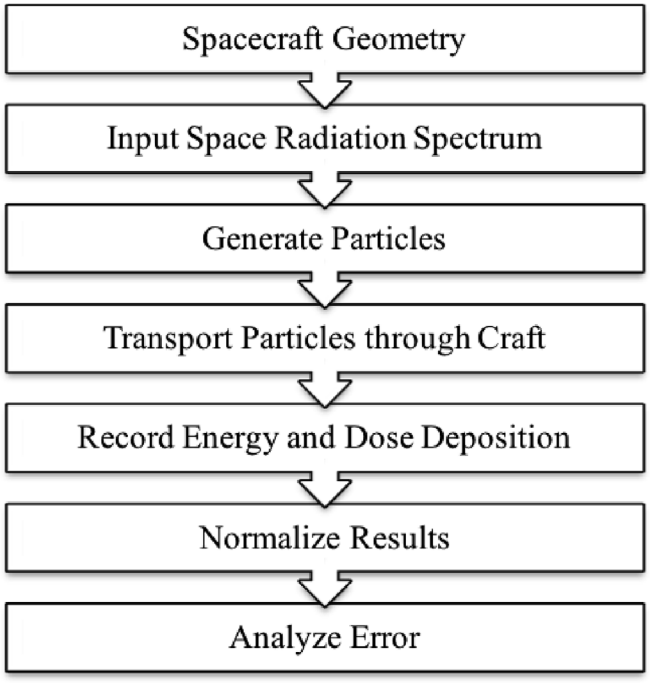

Fig. 1. GEANT4 steps: modeling of radiation transport through spacecraft aimed at radiation dose assessments.

shapes with Boolean operations and replicated volumes. This application uses the GEANT4 General Particle Source (GPS) [12], which allows for reading input spectra as macro files. The Space Environment Information System (SPENVIS) [13] generates the input particle spectra files based on mission time period and trajectory data. SPENVIS uses two line element trajectory paths to accurately generate ephemeris data and create spectra for each mission period.

GEANT4 contains many different built-in physics processes applicable to model radiation transport, which can be included in any model by the use of different physics lists. For modeling the space environment, there are four different physics lists: QGSP_BERT_HP, QGSP_BIC_HP, Shielding, and QBBC [14], which are selectable upon runtime. All four lists model the interactions as expected within the space radiation environment, including high-energy particles. The High Precision (HP) versions are selected when available to accurately model neutron transport from 10 GeV to thermal range. Spallation data in the space radiation environment energy range of 10 MeV–15 GeV show that the QGSP_BIC better matches experimental data for low energy protons and neutrons; whereas, QGSP_BERT better matches higher energy collisions [15]. The QBBC physics list combines the low energy BIC model, medium energy BERT model, and high energy QGSP and FTFP model; thus the QBBC list should better model the space environment.

The developed application in the simulation model includes GEANT4 command based scorer and multifunctional detectors. The multifunctional detector allows the use of many built-in scorers by attaching the scorer to a geometry volume, thus allowing scoring of multiple quantities simultaneously [16]. The simulation model includes an energy deposit scorer, dose deposit scorer, and three new dose equivalent scorers defined following the ICRP 60, 92, and 103 reports [17–19]. These dose equivalent scorers consist of three function files with associated headers. The scorers calculate the dose equivalent by finding the absorbed dose from a particle within a detector multiplied by the particle weighting factor for that type of radiation based on the ICRP standards.

When running a simulation, only enough particles are simulated to provide useful statistics, which is far less than the expected number of particles passing through the spacecraft over a given time interval. Thus

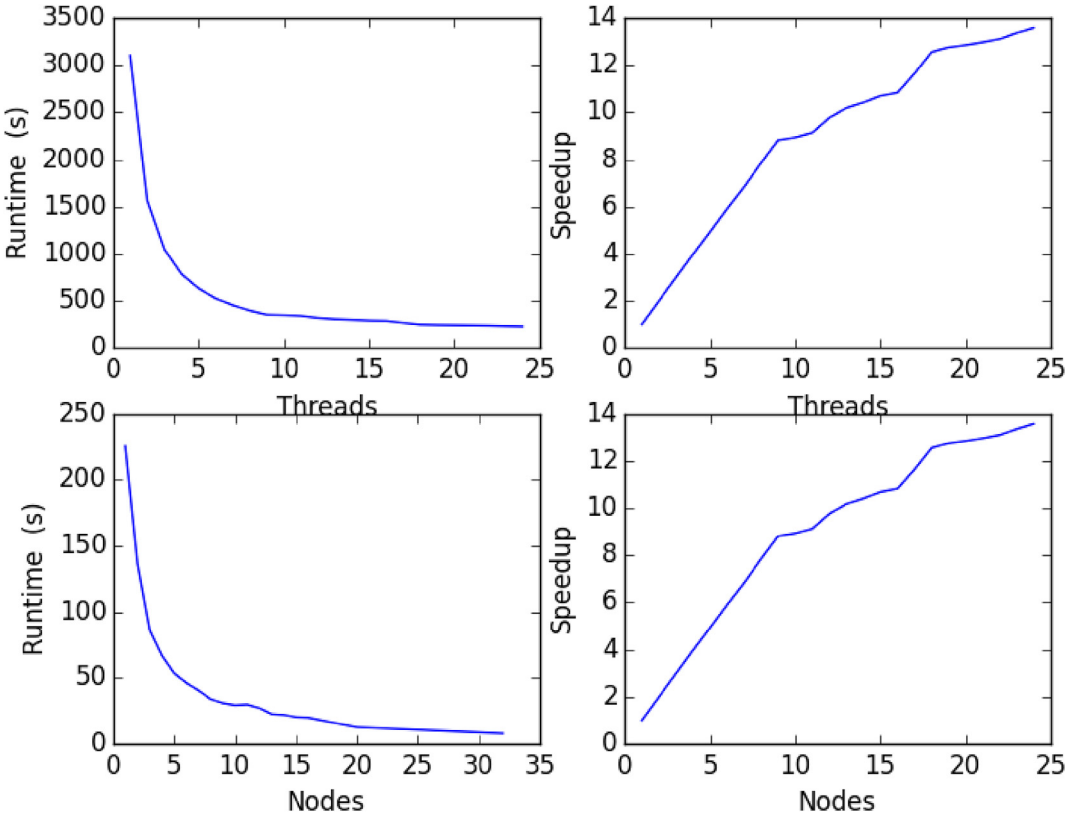

Fig. 2. Computation runtime and speedup for one million particles through a full-sized Apollo command module model of 15.8 m^3 with 20 GeV Protons versus the number of threads on a 2.8 GHz Intel Xeon Westmere X5660 processor and across varying number of nodes [10].

each scored quantity is multiplied by a normalization factor in order to normalize the values to the real-world number of particles expected to be passing through the spacecraft volume. The real scored value X_r is thus obtained as follows:

$$X_r = X_S \frac{N_r}{N_s} \tag{1}$$

where X_S is the scored quantity, N_s is the number of particles in the simulation, and N_r is the normalization factor. The normalization factor is dependent on the energy spectrum normalization factor n_1, the angular distribution of the particles from the source n_2, and the surface area of the spherical surface source S in cm^2 given by Ref. [20]:

$$N_r = n_1 n_2 S \tag{2}$$

For a given energy spectrum, the energy normalization factor n_1 is the integral fluence at the minimum energy minus the integral fluence at the maximum energy [21]. The angular distribution n_2 for a spherical surface source is dependent on the total radiation particles passing through the spherical surface, which is the total fluence for the time period. The total fluence $\Phi(T)$ in units of $MeV^{-1}cm^{-2}sr^{-1}$ for a spatially uniform radiation source independent of direction through the volume is found by integrating the directional flux $\phi(T, \omega, \phi)$ over the oblique angle θ from -1 to 1 and the solid angle ω from 0 to 2π:

$$\Phi(T) = \int_0^{2\pi} d\omega \int_{-1}^{1} \phi(T, \omega, \theta)\cos\theta d\theta = 4\pi\phi(T) \tag{3}$$

In the simulations, the GPS source creates particles around a spherical surface source, which is the vector current through the surface. Thus the angular distribution for a spherical surface source is dependent on the radiation current, not flux when normalizing results. The total current through the surface source into the spacecraft is a cosine law distribution:

$$j(T) = \int_0^{2\pi} d\omega \int_0^{1} \phi(T)\cos\theta d\theta = \pi\phi(T) \tag{4}$$

where $j(T)$ is the current and $\phi(T)$ is the directional fluence depending on energy T, oblique angle θ, and azimuthal angle ω. Thus solving Eq. (3) for $\phi(T)$ and substituting into Eq. (4) gives the current $j(T)$ through the source as 1/4 the total fluence [22].

$$j(T) = \frac{1}{4}\Phi_{4\pi}(T) \tag{5}$$

Thus the angular distribution factor n_2 for the simulations is 1/4.

GEANT4 does not track calculation error; therefore, it must be calculated manually. An error analysis module is therefore developed to automatically calculate standard deviation, relative error, and figure of merit similar to other Monte Carlo codes [23] for the quantities tallied. The standard deviation is the square root of the variance, which is the spread of the distribution for the tally. The relative error is the standard deviation divided by the mean. As the number of particles increases, the standard deviation decreases, reducing the relative error. Thus as the relative error decreases, the tally value approaches a nearly constant value [10]. For each simulation, between 500 million to 1 billion particles, depending on the size of the spacecraft, were simulated in every simulation to reduce the relative error to less than 5% for reliable simulations.

In order to reduce computational time, the developed new application in this simulation model includes multithreading based on either the POSIX standard [24] or C++11 threading in the latest release and MPI with event-level parallelism to break the total number of particles in a run between nodes and local threads equally. Thus, in a computational cluster, a master node sends copies of the simulation to each node to compute a subset of the total particles. At the end of the event run [25], the threads' and nodes' results are merged to the master node in a single tally outputted by the application as a comma separated

value file. The application was tested running on one node with one thread to 32 nodes with 216 simultaneous threads. The application had near linear speedup, shown in Fig. 2, which is a metric for the runtime of multiple threads divided by the runtime for a single thread. Fig. 2 also shows as the number of nodes increased, the speedup was not linear due to network communication and duplicating the simulation between the nodes; however, for a larger number of particles, the speedup would be closer to the number of nodes. Thus the application efficiently parallelized the simulations.

2.1. Creation of space radiation detector models

The presented new simulation model includes three comprehensive models of space radiation detectors defined in GDML for GEANT4 based on: International Commission on Radiation Units (ICRU) Phantom Sphere from the DESIRE project [26–28], Crew Personal Dosimeter (CPD), and a Tissue Equivalent Proportional Counter (TEPC). The GEANT4 detector models can be added to any spacecraft geometry. The ICRU phantom sphere model creates a 30 cm diameter tissue equivalent sphere, which mimics the radiation deposited within an astronaut.

The CPD, worn by astronauts to measure individual dose, contains 5 mm diameter cylinders of 1 mm thickness Thermoluminescent Detectors (TLD) embedded in a 4.5 cm by 3.5 cm Lexan holder [29]. The model includes 32 TLD-100 vol of 92.14% Lithium-6 fluoride and 7.26% Lithium-7 fluoride within a Lexan solid shown in Fig. 3.

The TEPC modeled was flown on STS-118 to the ISS in 2007 to provide active radiation monitoring. The simplified TEPC model of the detector for simulating GCR is made of four tubes: interior propane, plastic cylinder, vacuum cylinder, and a casing of 5.1 cm diameter. The outside casing is a vacuum chamber made of stainless steel. Inside is A-150 plastic with a density of 1.127 g/cm3 as shown in Fig. 4 [30]. The interior of the detector is filled with propane gas at a pressure of 15 Torr (2000 Pa).

2.2. GEANT4 simulation model of International Space Station

Simulations of the ISS were developed to validate this new GEANT4 based comprehensive simulation model against experimental data and previous studies regarding radiation shielding in space. Data for the ISS trajectory was based on NORAD's historical archive [31] TLE (Two Line Element) sets for the ISS during solar maximum in 2001 and solar minimum in 2009. The TLE sets were inputted into SPENVIS [21] to obtain ephemeris data and radiation spectra. The first set of simulations were aimed at validating the physics lists in comparing the QGSP_BIC_HP, QGSP_BERT_HP, and QBBC lists, using a detailed geometry model of the Columbus module with a truncated ISS model (col2iss1) from the DESIRE Project by Tori Ersmark [32]. The Columbus module contained 15 ICRU phantom spheres to calculate radiation dose, as shown in Fig. 5. The simulations used an AP-8 proton spectrum [33] from solar maximum between April and August 2001 at an altitude of 400 km [34] for comparison with results from the DESIRE Project.

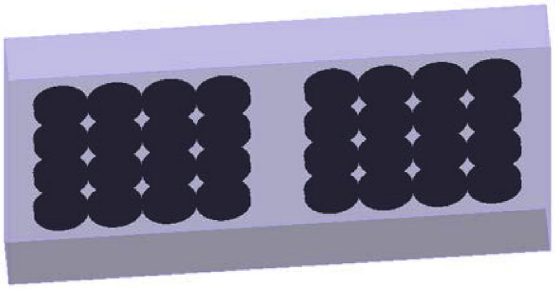

Fig. 3. Crew personal dosimeter model in GEANT4 with 32 TLD-100s detectors embedded in a Lexan holder.

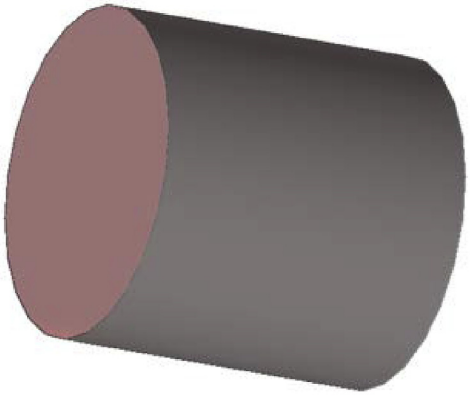

Fig. 4. Simplified TEPC detector model in GEANT4 made of four cylindrical layers.

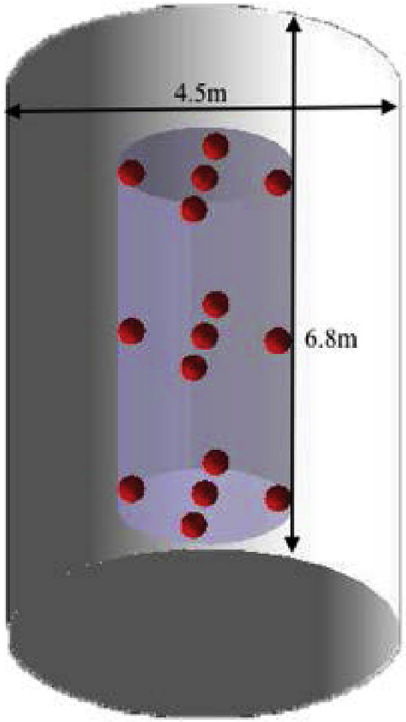

Fig. 5. GEANT4 model of the Columbus module with 15 ICRU phantom spheres from DESIRE project [35].

The next series of simulations compared the dose rate for the solar maximum in 2001, using all nine DESIRE Project geometry models, which contained increasingly detailed models of the Columbus module with and without the ISS. The first Columbus module model (col0) was a simplified model with 10 vol with 25% of the total mass of the module. The second model (col2) had 23 vol with a correct total mass and simplified equipment racks. The third model (col3) had 750 vol to more precisely model the interior racks. The Columbus models were combined with a truncated ISS (iss1) model, a full ISS model (iss2), and without an ISS model (iss0).

Subsequent simulations, during solar maximum from June through July 2009, calculated the trapped radiation dose and dose equivalent, using the ICRP 60, 92, and 103 scorers with the col3iss1 model. Then a series of simulations were developed to calculate the GCR dose contribution for all ions from hydrogen through iron, during solar maximum in 2001 and solar minimum in 2009. The GCR spectra were generated in SPENVIS, using the ISO-15390 and ISO-15390 + 1 sigma

standard deviation model in SPENVIS [36–38]. The GCR simulations used the detailed Columbus model with truncated ISS and were compared with simulations using the same geometry from the DESIRE Project and Chavy-Macdonald et al. [27,39].

2.3. GEANT4 simulation model of The Apollo 11 and Apollo 14 command modules

Being the only human-crewed missions beyond LEO, the Apollo missions provided unique information about radiation doses received by astronauts in deep space. A GEANT4 model was developed to simulate Apollo 11 and Apollo 14 missions, based on a newly created GEANT4 geometry command module (CM) model. The CM model consisted of an inner shell of aluminum honeycomb in-between two aluminum plates and an outer shell of steel honeycomb between two plates. In the middle of the shells was a 3.5 lb/ft2 density fibrous insulation [40]. Outside the outer shell was an ablative heat shield with up to 27 layers of Kapton for thermal insulation. The CM capsule was broken into four sections: a central heat shield, an aft heat shield, a forward heat shield, and a top hatch, consisting of the following multiple layers: Kapton, ablator, stainless steel plates and honeycomb, insulation, aluminum plates and honeycomb, interior, and equipment racks. The CM was built from a polycone structure for the central heat shield combined with Boolean operations to form the spherical aft heat shield with a diameter of 154". The central heat shield with a polycone shape extended to the top forward hatch narrowing towards the top. The forward heat shield consisted of a polycone that fit on the outside of the central heat shield to the top hatch. The inside of the space capsule was filled with air and either 15 ICRU spheres as shown in Fig. 6 or a human anatomical phantom to score the dose deposition within the tissue.

Two GEANT4 models of the Apollo CM were developed. The first model, CM 1, consisted of a simplified geometry, including only structural layers. The second model CM 2, included additional equipment racks inside the interior of the capsule made of aluminum to correctly match the weight of the CM and extra shielding from interior equipment racks. The first model had a mass of 1566 kg that was far less than the 5809 kg of the actual CM, so the second model added equipment racks of aluminum with a density equal to the difference in this mass divided by the volume of the equipment racks.

From Trans Lunar Injection (TLI) data and Trans-Earth Injection (TEI) data [10,41,42], the trajectory of both Apollo 11 and Apollo 14 were calculated in the Geocentric Equatorial Inertial System (GEI) coordinates, using NASA's General Mission Analysis Tool (GMAT) [43]. The trajectories were verified for both missions by comparison with published lunar locations in GEI coordinates [10]. The GEI coordinates were then inputted into SPENVIS [13] to generate trapped proton and electron fluence for the radiation belts. The fluence was trajectory

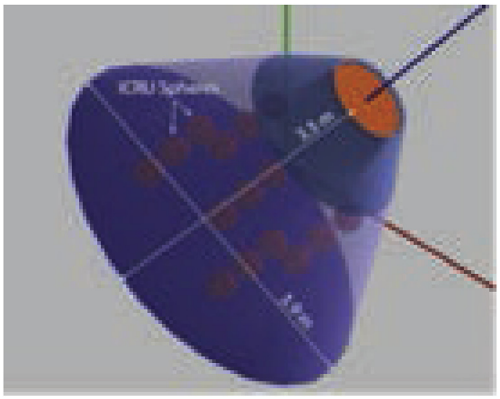

Fig. 6. GEANT4 Apollo command module geometry with 15 ICRU tissue equivalent spheres located inside.

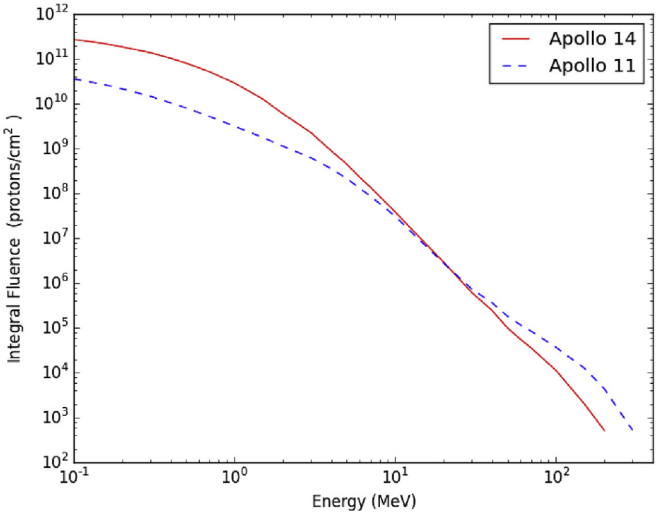

Fig. 7. Integral proton fluence vs. energy (MeV) for Apollo 11 and Apollo 14 outbound trapped protons in the radiation belts generated from trajectory calculations input into SPENVIS [21].

dependent affecting the spacecraft for a few hours during the short outbound and inbound legs of the trans-lunar voyage. Fig. 7 shows the total proton fluence for the outbound leg from the AP-8 model [33,44] versus proton energy for Apollo 11 and Apollo 14. Apollo 14 had a lower high-energy fluence than Apollo 11 with higher low-energy fluence. Since the hull easily stopped low energy as opposed to high energy, the dose from trapped protons was lower for Apollo 14 then Apollo 11. Apollo 14 had a higher electron fluence due to the trajectory through the electron radiation belt. Since the Apollo hull easily stopped low energy electrons, the electron fluence for Apollo 11 resulted in low dose to Apollo 11 astronauts, but not Apollo 14 due to higher energy electron fluence.

Apollo 11 in 1969 and Apollo 14 in 1971 took place during solar maximum, which reduced the GCR fluence. Thus the Nymmik et al. model [45] was used to generate the GCR spectra for all ions from hydrogen through iron at a distance of one astronomical unit in free-space. The ion spectra were similar between both missions except for a slight increase for low energy hydrogen ions for Apollo 14, due to the later mission time period in the solar cycle.

The Apollo missions occurred during solar maximum in solar cycle twenty; thus the Apollo missions were likely to experience a SPE. Only Apollo 12 detected a small SPE by external instrumentation with no increased dose inside the capsule [46]. To understand what the effects of a SPE would have been on astronaut dose within the Apollo command module, models of historical SPEs were simulated, including two historical SPE events in SPENVIS: ESP-PYSCHIC (Emission of Solar Protons - Prediction of Solar particle Yields for CHaracterizing Integrated Circuits) worst-case [47] and Johnson Propulsion Lab-91 (JPL-91). The ESP-PSYCHIC models are an empirical fit to the solar proton fluence from solar cycle 20–22 with the worst-case model predicting the maximum fluence, including the largest recorded SPEs. The JPL model is the abnormally large SPE event took place in 1972 and typically referred to as King SPE. Fig. 8 shows the differential flux for the two worst-case scenarios SPEs as if they would have occurred when the Apollo spacecraft was outside Earth's protective magnetosphere.

3. Analysis of the radiation dose in the GEANT4 space simulation models

3.1. GEANT4 model of the ISS dose during solar minimum and solar maximum

The simulations, using the three different GEANT4 physics lists, of

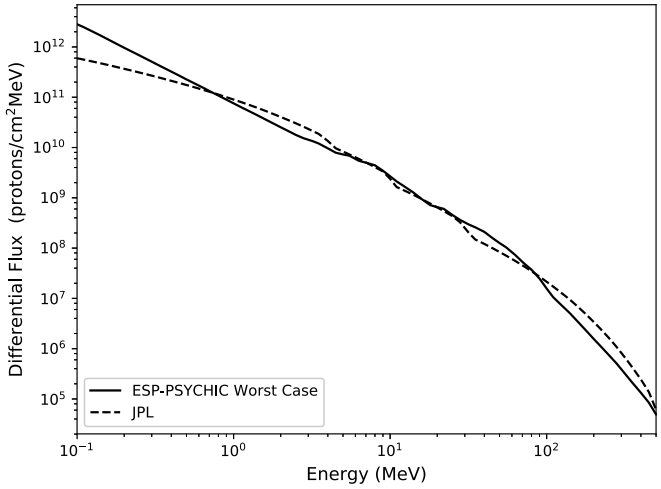

Fig. 8. Differential flux for historical SPE events vs. energy (MeV) at 1 AU from Earth.

solar maximum in 2001 for trapped protons showed that all of them resulted in similar dose and dose equivalents rates within 1%. The run-time for the QGSP_BERT_HP and QGSP_BIC_HP lists were the longest at 37.3 and 37.7 h respectively for 2.1 billion particles, due to the high precision neutron libraries [48]. The run-time for 2.1 billion particles, using the QBBC physics list, was 35.4 h. Thus, the QBBC physics list was used for all further simulations, since it resulted in similar results to the other physics lists with a shorter runtime.

The calculated quality factor was 4.7 for the ICRP-60 scorer, which was significantly higher than the measured quality factor from DOSTEL and TEPC detectors onboard the ISS [34]. The ICRP-60 publication recommended that protons with energies higher than 2 MeV have a weighting factor of 5 compared to a weighting factor of 2 in ICRP-92 and ICRP-103, greatly overestimating the dose equivalent. Table 1 compares the dose equivalent rates for ICRP-60, ICRP-92, and ICRP-103, caused by different weighting factors. The ICRP-103 scorer was used for further simulations, since the ICRP-103 scorer was closer to DOSTEL and TEPC dose equivalents.

Table 2 shows a comparison of the different Columbus geometry models from the DESIRE project for solar maximum in 2001, using the AP-8 trapped proton model. The first Columbus model with no ISS (col1iss0) shows the greatest dose due to the smaller shielding density. The addition of the truncated (iss0) or full ISS (iss1) model reduced the dose, because of increased shielding for a large solid angle, similar to results obtained from the DESIRE project [28] by Ersmark. The variation between the two ISS models, full ISS and truncated ISS, was smaller than the standard deviation between ICRU spheres within the Columbus module itself, confirming Ersmark's assumption that a truncated geometry accurately models the full station geometry without the needed computational overhead of a full-sized ISS model [28].

The second Columbus model (col2) shows a lower dose rate than the more detailed third Columbus model (col3) because of secondary particles from the additional shielding. The third Columbus model with truncated geometry (col3iss1) tallied a dose of 75 μGy/day for trapped protons versus the similar earlier work by Ersmark of 79 μGy/day. This simulation with truncated geometry required 4 h 36 min of computation time on a 2.8 GHz Intel Xeon Westmere X5660 processor with 12 threads, 9.2 CPU days, whereas for the DESIRE project it required over 40 computation days [32]. During the same time period in similarly shielded areas onboard the ISS, the DOSTEL detector recorded a dose of 102 μGy/day, and the TEPC recorded a dose of 74 μGy/day [34].

Table 1
Simulated dose and dose equivalent rates for ICRP-60, ICRP-92, and ICRP-103 standards for the Columbus module with the truncated ISS model, using an AP-8 trapped proton spectrum, during solar maximum in 2001.

ICRP Standard	Dose (μGy/day)	Quality Factor	Dose Equivalent (μSv/day)
ICRP-60	75.2	4.7	356
ICRP-92	75.2	2.0	155.8
ICRP-103	75.2	2.0	155.9

Table 2
Comparison of the dose deposition for the three Columbus models with different ISS models for trapped protons, during solar maximum in 2001.

Columbus Geometry Model	Dose (μGy/day)	Standard Deviation Across ISS Module (μGy/day)
col1iss0	269	11.4
col1iss1	219	21.2
col1iss2	214	43.6
col2iss0	85.3	18.9
col2iss1	59.3	6.6
col2iss2	63.5	15.4
col3iss0	88.9	28.4
col3iss1	75.2	16.0
col3iss2	70.8	8.6

The GEANT4 simulation of trapped protons during solar minimum in 2009 resulted in a dose rate of 95.2 μGy/day, which fell within measured values from the DOSTEL experiment of 120–95 μGy/day [49] and below the TEPC measured data of 109 μGy/day [50,51], as well as previous simulations by Chavey-McDonald, Ersmark, and ESA by sectoring, shown in Fig. 9 [39]. The GEANT4 simulations were less than the DESIRE and ESA sectoring values, but higher then simulations by Chavey-McDonald.

Simulations of the GCR total dose rate from all hydrogen through iron ions with the ISO-15390 model, during solar maximum in 2001, resulted in a dose of 75.9 μGy/day with a dose equivalent of 313 μSv/day. The dose rate was within the range of values from the two GCR models simulated by the DESIRE project of 99 μGy/day for the SIREST model and 63 μGy/day for the CREME96 model [27], but were less than the measured value of 92 μGy/day from DOSTEL and 91 μGy/day from TEPC [34] as shown in Fig. 10. However, simulations with the ISO-15390 + 1 sigma model resulted in a dose rate of 94 μGy/day with a dose equivalent of 362 μSv/day, which better matches the experimental data. ISO-15390 + 1 sigma model included the particle fluence within one standard deviation of the GCR spectra, thus in future simulations, the +1 sigma model better matches possible GCR spectra. The quality factor for the GCR only simulations was 3.8, which was in the range of

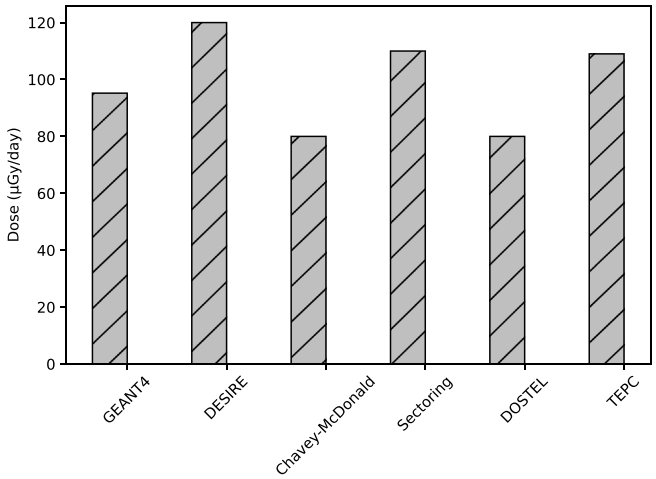

Fig. 9. Comparison of GEANT4 dose rates, during solar minimum in 2009, with values from the DESIRE project, Chavey-McDonald, ESA Sectoring, and experimental data from DOSTEL and TEPC [34,39].

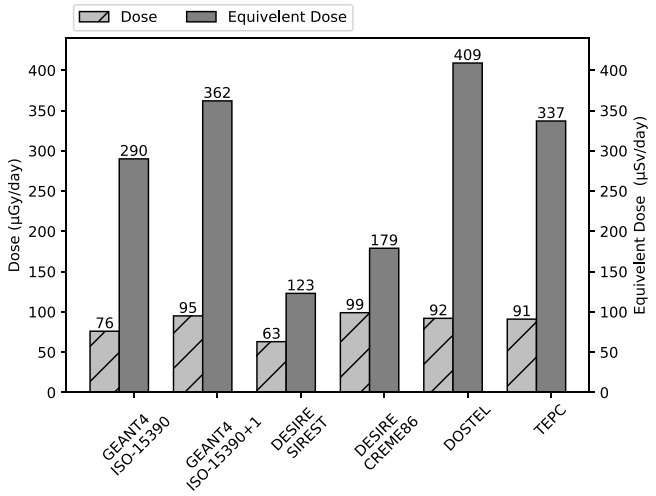

Fig. 10. Comparison of GEANT4 dose and dose equivalent rates for ISO-15390 model and ISO-15390 + 1, during solar maximum in 2001, with results by the DESIRE project and measured DOSTEL and TEPC data.

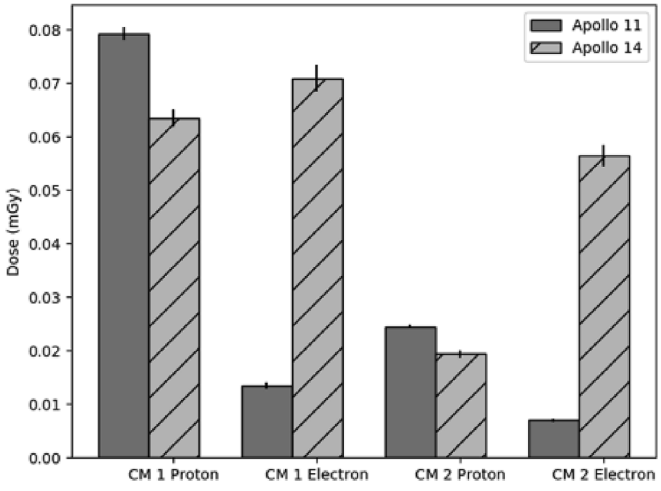

Fig. 11. Trapped proton and electron dose in command modules with the simulation relative error for Apollo 11 and Apollo 14 missions obtained with GEANT4 models.

Table 3
Comparison of GEANT4 dose rate values by Apollo CM model for different GCR ions.

Model	Ion	Dose (μGy/day)	Relative Error
CM 1	H	121	1.26%
CM 2	H	149	1.01%
CM 1	He	13.6	1.20%
CM 1	Li	.0512	1.17%
CM 1	Be	.0350	1.16%
CM 1	C	.380	1.20%
CM 1	O	.365	1.22%

Table 4
Apollo 11 and Apollo 14 mission dose from trapped radiation belts, GCR, total dose (trapped and GCR), and the total measured mission dose.

Apollo Mission	Trapped (mGy)	GCR (mGy)	Total (mGy)	Measured Dose (mGy) [3]
11	.093	1.30	1.39	1.8
14	.134	1.46	1.60	11.4

the DOSTEL quality factor of 4.4 and TEPC quality factor of 3.7 measured by Reitz et al. for GCR, during solar maximum in 2001 [34].

3.2. GEANT4 dose analysis for Apollo 11 and Apollo 14 missions

CM 1 model simulations resulted in double the dose for trapped protons and electrons than CM 2 because of the added shielding from equipment racks in the hull of CM 2. The proton dose for Apollo 11 was higher than the dose from electrons; however, the electron dose and total dose for Apollo 14 was higher due to the longer trajectory through the outer trapped electron radiation belt, shown in Fig. 11 with relative simulation errors. Since Apollo 14 was a longer duration mission, the total simulated dose for GCR was higher than for Apollo 11 even though both missions had similar GCR dose. The most significant contributor to the GCR dose was from hydrogen ions followed by helium ions, shown in Table 3. The CM 2 model had a larger dose from GCR hydrogen ions then CM 1, because the increased shielding from CM 2 caused more secondary radiation.

The simulated total dose for Apollo 11 was 1.39 mGy from both trapped protons and GCR, which was within 24% relative error of the mission-recorded dose, shown in Table 4. The Apollo 14 simulation showed the total dose value to be an order of magnitude less than the measured value, but higher than Apollo 11. The increased simulated dose was due to greater trapped electron dose and the increased mission length, which resulted in an increased GCR dose. The standard deviations between the fifteen ICRU spheres across the capsule for trapped protons, trapped electrons, and GCR were less than the simulated dose by an order of magnitude smaller; thus spatial distribution within the capsule did not explain the significantly higher increased dose for Apollo 14. The difference in the spacecraft trajectories through the radiation belts for the missions did not explain why the Apollo 14 proton dose rate was higher than Apollo 11 by an order of magnitude.

The simulated dose from historical SPE models were lower than the mission maximum dose of 4 Gy for astronauts within the craft, shown in Table 5; however, the dose would have been higher if astronauts were in a thinner shielded lunar module or a spacesuit. The CM 2 model with additional shielding from equipment racks reduced the radiation dose by a third from the simplified CM 1 model, thus small amounts of additional shielding in future missions would significantly reduce SPE doses. The simulations showed that a SPE would result in a significant dose but not enough to cause acute radiation sickness. The relative simulation error was low due to a high number of simulated particles. The standard deviations between the fifteen ICRU spheres was well below the average dose, thus showing an order of magnitude smaller variation in the radiation dose within the capsule. The JPL model showed the highest deposited dose over the ESP-PYSCH-Worst case spectrum.

The calculated dose for the human trunk in the anatomical model within the CM showed close agreement to the ICRU spheres; however, human organ doses varied greatly, as shown in Fig. 12. The human phantom was placed within the CM with the head towards the forward hatch, so there was less shielding for the upper body than the lower body, resulting in the higher dose distribution for those organs in the simulation. Thus the skull received the highest dose of any organ for both missions, followed by the brain, upper spine, and arm bones.

4. Conclusion

The new GEANT4 based application developed successfully implemented MPI and multithreading, providing significantly reduced runtime for simulations. All three physics lists available in the GEANT4 based application, i.e., QBBC, QGSP_BIC_HP, and QGSP_BERT_HP show close agreement in values when analyzing the effect of trapped protons on the ISS. The QBBC physics list uses less computation time than the other physics lists for simulations of the space environment. The developed ICRP-92 and ICRP-103 dose equivalent scorers for GEANT4

Table 5
Comparison of radiation dose by historical SPE events for the two CM models.

Model	Spectrum	Dose (mGy)	Relative Error	Standard Deviation (mGy)
CM 1	ESP-PYSCH Worst	521	0.5%	67.8
CM 2	ESP-PYSCH Worst	169	0.7%	47.0
CM 1	JPL	884	0.3%	71.3
CM 2	JPL	319	0.3%	65.3

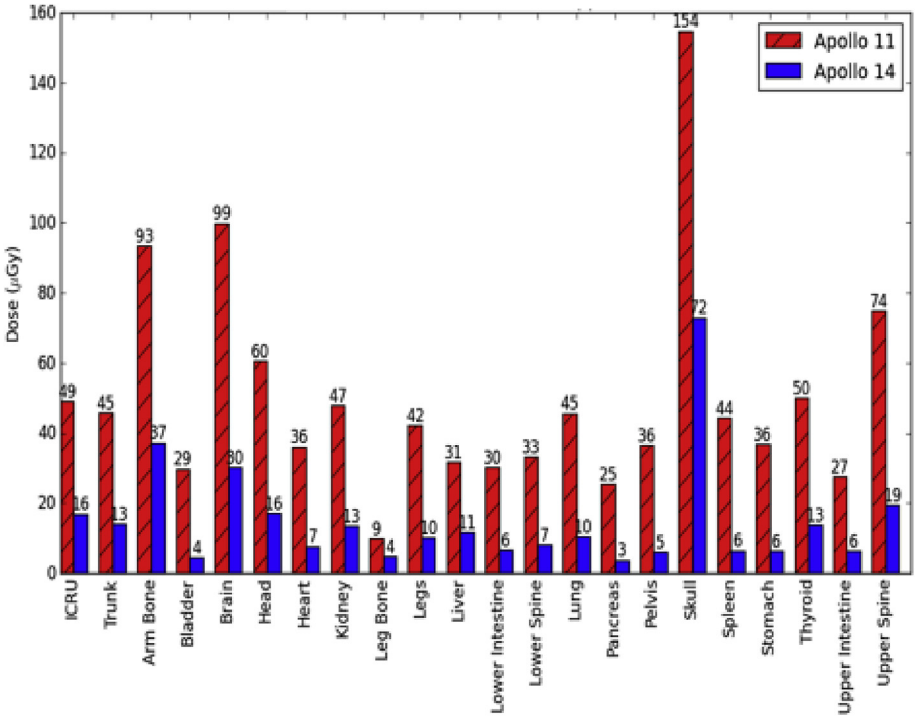

Fig. 12. GEANT4 calculated human phantom radiation dose by organ for Apollo 11 and Apollo 14 missions from trapped protons.

resulted in quality factors close to the experimentally measured quality factors for GCR and trapped proton spectrum, whereas the scorer based on the ICRP-60 report greatly overestimates the dose equivalent.

The calculated radiation dose rate onboard the ISS from the GEANT4 based models correlated with experimental data from ISS detectors. These GEANT4 simulations take less computational time than the earlier simulations from the DESIRE Project. The simulated trapped proton dose, during solar maximum and minimum, is within experimental data ranges; however, the GCR simulations using the ISO 15390 model are less than experimentally measured values. Thus, future simulations of GCR dose require more accurate GCR spectra models, such as using the ISO 15390 + 1 sigma model.

The simulation of the Apollo 11 mission resulted in a radiation dose close to the experimental data; however, the GEANT4 calculated trapped proton and electron dose for Apollo 14 mission is less than Apollo 11. The Apollo 14 total dose is higher than the Apollo 11 dose due to increased mission length, causing more exposure to GCR. The GEANT4 calculated values are still an order of magnitude smaller than the measured dose values. The spatial distribution in dose is small, thus spatial variations do not explain the order of magnitude higher dose nor do the trajectory through the radiation belts. Simulations of the two SPE models for the Apollo models show that a large SPE event would not be fatal and below mission limits.

Because of the variation in results between the geometry models in this article, more accurate simulations of future deep-space missions will require more precise spacecraft geometry models from Computer Aided Design (CAD) detailed drawings with improved radiation environment models.

Acknowledgments

We gratefully acknowledge the support and resources from the Center for High-Performance Computing at the University of Utah, the online European Space Agency SPENVIS database and NASA OLTARIS database used to access radiation environment models, and CelesTrak for TLE element data.

We are grateful to Dr. Tori Ersmark for his GDML models of ISS from the DESIRE project and Dr. Eric Benton from Oklahoma State University for Apollo mission dose data and his correspondence.

This research was supported and funded by the Utah Nuclear Engineering Program and the Nuclear Regulatory Commission Fellowship.

References

[1] E.R. Benton, E.V. Benton, Space radiation dosimetry in low-earth orbit and beyond, Nucl. Instrum. Methods Phys. Res. Sect. B Beam Interact. Mater. Atoms 184 (1–2) (2001) 255–294, https://doi.org/10.1016/s0168-583x(01)00748-0.

[2] G.D. Badhwar, Shuttle radiation dose measurements in the international space station orbits, Radiat. Res. 157 (1) (2002) 69–75, https://doi.org/10.2307/3580854 http://www.jstor.org/stable/3580854.

[3] R.A. English, R.E. Benson, J.V. Bailey, C.M. Barnes, Apollo Experience Report: Protection against Radiation, Report, National Aeronautics and Space Administration, 1973.

[4] J.W. Wilson, F.F. Badavi, F.A. Cucinotta, J.L. Shinn, G.D. Badhwar, R. Silberberg, C. Tsao, L.W. Townsend, R.K. Tripathi, Hzetrn: Description of a Free-Space Ion and Nucleon Transport and Shielding Computer Program, (1995).

[5] R.C. Singleterry, S.R. Blattnig, M.S. Clowdsley, G.D. Qualls, C.A. Sandridge, L.C. Simonsen, J.W. Norbury, T.C. Slaba, S.A. Walker, F.F. Badavi, J.L. Spangler, A.R. Aumann, E.N. Zapp, R.D. Rutledge, K.T. Lee, R.B. Norman, Oltaris: On-Line Tool for the Assessment of Radiation in Space, Report NASA/TP-2010-216722

NASA Langley Research Center, 2010 Jul 01, 2010.
[6] F. Lei, P.R. Truscott, C.S. Dyer, B. Quaghebeur, D. Heynderickx, P. Nieminen, H. Evans, E. Daly, Mulassis: a geant4-based multilayered shielding simulation tool, IEEE Trans. Nucl. Sci. 49 (6) (2002) 2788–2793, https://doi.org/10.1109/tns.2002.805351.
[7] G. Santin, V. Ivanchenko, H. Evans, P. Nieminen, E. Daly, Gras: a general-purpose 3-d modular simulation tool for space environment effects analysis, IEEE Trans. Nucl. Sci. 52 (6) (2005) 2294–2299, https://doi.org/10.1109/tns.2005.860749.
[8] S. Agostinelli, J. Allison, K. Amako, J. Apostolakis, H. Araujo, P. Arce, M. Asai, D. Axen, S. Banerjee, G. Barrand, F. Behner, L. Bellagamba, J. Boudreau, L. Broglia, A. Brunengo, H. Burkhardt, S. Chauvie, J. Chuma, R. Chytracek, G. Cooperman, G. Cosmo, P. Degtyarenko, A. Dell'Acqua, G. Depaola, D. Dietrich, R. Enami, A. Feliciello, C. Ferguson, H. Fesefeldt, G. Folger, F. Foppiano, A. Forti, S. Garelli, S. Giani, R. Giannitrapani, D. Gibin, J.J. Gómez Cadenas, I. González, G. Gracia Abril, G. Greeniaus, W. Greiner, V. Grichine, A. Grossheim, S. Guatelli, P. Gumplinger, R. Hamatsu, K. Hashimoto, H. Hasui, A. Heikkinen, A. Howard, V. Ivanchenko, A. Johnson, F.W. Jones, J. Kallenbach, N. Kanaya, M. Kawabata, Y. Kawabata, M. Kawaguti, S. Kelner, P. Kent, A. Kimura, T. Kodama, R. Kokoulin, M. Kossov, H. Kurashige, E. Lamanna, T. Lampén, V. Lara, V. Lefebure, F. Lei, M. Liendl, W. Lockman, F. Longo, S. Magni, M. Maire, E. Medernach, K. Minamimoto, P. Mora de Freitas, Y. Morita, K. Murakami, M. Nagamatu, R. Nartallo, P. Nieminen, T. Nishimura, K. Ohtsubo, M. Okamura, S. O'Neale, Y. Oohata, K. Paech, J. Perl, A. Pfeiffer, M.G. Pia, F. Ranjard, A. Rybin, S. Sadilov, E. Di Salvo, G. Santin, T. Sasaki, N. Savvas, Y. Sawada, et al., Geant4—a simulation toolkit, Nucl. Instrum. Methods Phys. Res. Sect. A Accel. Spectrom. Detect. Assoc. Equip. 506 (3) (2003) 250–303 https://doi.org/10.1016/S0168-9002(03)01368-8 http://www.sciencedirect.com/science/article/pii/S0168900203013688.
[9] J. Allison, K. Amako, J. Apostolakis, P. Arce, M. Asai, T. Aso, E. Bagli, A. Bagulya, S. Banerjee, G. Barrand, B.R. Beck, A.G. Bogdanov, D. Brandt, J.M. Brown, H. Burkhardt, P. Canal, D. Cano-Ott, S. Chauvie, K. Cho, G.A. Cirrone, G. Cooperman, M.A. Cortés-Giraldo, G. Cosmo, G. Cuttone, G. Depaola, L. Desorgher, X. Dong, A. Dotti, V.D. Elvira, G. Folger, Z. Francis, A. Galoyan, L. Garnier, M. Gayer, K.L. Genser, V.M. Grichine, S. Guatelli, P. Guèye, P. Gumplinger, A.S. Howard, I. Hřivnáčová, S. Hwang, S. Incerti, A. Ivanchenko, V.N. Ivanchenko, F.W. Jones, S.Y. Jun, P. Kaitaniemi, N. Karakatsanis, M. Karamitrosi, M. Kelsey, A. Kimura, T. Koi, H. Kurashige, A. Lechner, S.B. Lee, F. Longo, M. Maire, D. Mancusi, A. Mantero, E. Mendoza, B. Morgan, K. Murakami, T. Nikitina, L. Pandola, P. Paprocki, J. Perl, I. Petrović, M.G. Pia, W. Pokorski, J.M. Quesada, M. Raine, M.A. Reis, A. Ribon, A. Ristić Fira, F. Romano, G. Russo, G. Santin, T. Sasaki, D. Sawkey, J.I. Shin, I.I. Strakovsky, A. Taborda, S. Tanaka, B. Tomé, T. Toshito, H.N. Tran, P.R. Truscott, L. Urban, V. Uzhinsky, J.M. Verbeke, M. Verderi, B.L. Wendt, H. Wenzel, D.H. Wright, D.M. Wright, T. Yamashita, J. Yarba, H. Yoshida, Recent developments in GEANT4, Nucl. Instrum. Methods Phys. Res. Sect. A Accel. Spectrom. Detect. Assoc. Equip. 835 (2016) 186–225, https://doi.org/10.1016/j.nima.2016.06.125 https://www.sciencedirect.com/science/article/pii/S0168900216306957.
[10] M. Lund, High-performing Simulations of the Space Radiation Environment for the International Space Station and Apollo Missions, Thesis (2016).
[11] R. Chytracek, J. McCormick, W. Pokorski, G. Santin, Geometry description markup language for physics simulation and analysis applications, IEEE Trans. Nucl. Sci. 53 (5) (2006) 2892–2896, https://doi.org/10.1109/TNS.2006.881062 http://ieeexplore.ieee.org/ielx5/23/36085/01710291.pdf?tp=&arnumber=1710291&isnumber=36085.
[12] C. Ferguson, General Purpose Source Particle Module for geant4 Sparset: Technical Note, Uos-GSPM-Tech, 2000 1.0.
[13] D. Heynderickx, B. Quaghebeur, E. Speelman, E. Daly, ESA's Space Environment Information System (SPENVIS) - a WWW interface to models of the space environment and its effects, Aerospace Sciences Meetings, American Institute of Aeronautics and Astronautics, 2000, , https://doi.org/10.2514/6.2000-371 10.2514/6.2000-371 https://doi.org/10.2514/6.2000-371.
[14] D. Wright, A short guide to choosing a physics list, Geant4 Tutorial at Marshall Space Flight Center, SLAC, 2012, http://geant4.slac.stanford.edu/MSFC2012/ChoosePhys.pdf.
[15] A.V. Ivantchenko, V.N. Ivanchenko, J.M. Molina, S.L. Incerti, Geant4 hadronic physics for space radiation environment, Int. J. Radiat. Biol. 88 (1–2) (2012) 171–175, https://doi.org/10.3109/09553002.2011.610865 http://www.ncbi.nlm.nih.gov/pubmed/21830895.
[16] J. Allison, K. Amako, J. Apostolakis, H. Araujo, P. Arce Dubois, M. Asai, G. Barrand, R. Capra, S. Chauvie, R. Chytracek, G.A.P. Cirrone, G. Cooperman, G. Cosmo, G. Cuttone, G.G. Daquino, M. Donszelmann, M. Dressel, G. Folger, F. Foppiano, J. Generowicz, V. Grichine, S. Guatelli, P. Gumplinger, A. Heikkinen, I. Hrivnacova, A. Howard, S. Incerti, V. Ivanchenko, T. Johnson, F. Jones, T. Koi, R. Kokoulin, M. Kossov, H. Kurashige, V. Lara, S. Larsson, F. Lei, O. Link, F. Longo, M. Maire, A. Mantero, B. Mascialino, I. McLaren, P. Mendez Lorenzo, K. Minamimoto, K. Murakami, P. Nieminen, L. Pandola, S. Parlati, L. Peralta, J. Perl, A. Pfeiffer, M.G. Pia, A. Ribon, P. Rodrigues, G. Russo, S. Sadilov, G. Santin, T. Sasaki, D. Smith, N. Starkov, S. Tanaka, E. Tcherniaev, B. Tome, A. Trindade, P. Truscott, L. Urban, M. Verderi, A. Walkden, J.P. Wellisch, D.C. Williams, D. Wright, H. Yoshida, Geant4 developments and applications, IEEE Trans. Nucl. Sci. 53 (1) (2006) 270–278, https://doi.org/10.1109/tns.2006.869826.
[17] ICRP, Icrp publication 60: 1990 recommendations of the international commission on radiological protection, Ann. ICRP 60 (1990).
[18] J. Valentin, Icrp publication 92: relative biological effectiveness (rbe), quality factor (q), and radiation weighting factor (wr): approved by the commission in january 2003, Ann. ICRP 33 (4) (2003) 1–121.
[19] J. Valentin, Icrp publication 103: the 2007 recommendations of the international commission on radiological protection, Ann. ICRP 103 (2007), https://doi.org/10.1097/01.HP.0000324200.73903.5b.
[20] G. Falzetta, F. Longo, A. Zanini, Geant4 and creme96 comparison using only proton fluxes, http://arxiv.org/abs/0712.2149v2, (2008).
[21] Belgian Institute for Space Aeronomy, Space Environment Information System (Spenvis), (2015) https://www.spenvis.oma.be.
[22] S.M. Seltzer, Conversion of depth-dose distributions from slab to spherical geometries for space-shielding applications, IEEE Trans. Nucl. Sci. 33 (6) (1986) 1292–1297, https://doi.org/10.1109/TNS.1986.4334595.
[23] Monte Carlo Team, Mcnp–A General Monte Carlo N-Particle Transport Code, Los Alamos National Lab, 20085.
[24] D. Xin, C. Gene, A. John, J. Sverre, N. Andrzej, A. Makoto, B. Daniel, Creating and improving multi-threaded geant4, J. Phys. Conf. Ser. 396 (5) (2012) 052029http://stacks.iop.org/1742-6596/396/i=5/a=052029.
[25] R.-k. Dai, J.-x. Li, L. Li, C.-l. Dong, B. Yan, A Parallel Monte Carlo Simulation on Cluster System for Particle Transport, (2009), pp. 31–35, https://doi.org/10.1109/aici.2009.485.
[26] T. Ersmark, P. Carlson, E. Daly, C. Fuglesang, I. Gudowska, B. Lund-Jensen, P. Nieminen, M. Pearce, G. Santin, Geant4 Monte Carlo simulations of the belt proton radiation environment on board the international space station/columbus, IEEE Trans. Nucl. Sci. 54 (4) (2007) 1444–1453, https://doi.org/10.1109/tns.2007.896344.
[27] T. Ersmark, P. Carlson, E. Daly, C. Fuglesang, I. Gudowska, B. Lund-Jensen, P. Nieminen, M. Pearce, G. Santin, Geant4 Monte Carlo simulations of the galactic cosmic ray radiation environment on-board the international space station/columbus, IEEE Trans. Nucl. Sci. 54 (5) (2007) 1854–1862, https://doi.org/10.1109/tns.2007.906276.
[28] T. Ersmark, P. Carlson, E. Daly, C. Fuglesang, I. Gudowska, B. Lund-Jensen, P. Nieminen, M. Pearce, G. Santin, Influence of geometry model approximations on geant4 simulation results of the columbus/iss radiation environment, Radiat. Meas. 42 (8) (2007) 1342–1350 https://doi.org/10.1016/j.radmeas.2007.06.001 http://www.sciencedirect.com/science/article/pii/S1350448707002879.
[29] E. Semones, Report, NASA- Johnson Space Center, (Dec 8 1999) https://www.nasa.gov/centers/johnson/pdf/514208main_ES-01_Passive_Dosimetry_Area_%26_Crew_Monitoring_E.Semones.pdf.
[30] E. Semones, Update on nasa tepc activities september 08–september 09, 14th Workshops on Radiation Monitoring for the International Space Station, Dublin, 2010 http://wrmiss.org/workshops/fourteenth/Semones.pdf.
[31] T. Kelso, Norad two-line element sets historical archives, online database, Celestrak, http://www.celestrak.com/NORAD/archives/request.asp , Accessed date: 22 December 2004.
[32] T. Ersmark, Geant4 Monte Carlo Simulations of the International Space Station Radiation Environment, Thesis KTH, Stockholm, 2006.
[33] D.M. Sawyer, J.I. Vette, Ap-8 Trapped Proton Environment for Solar Maximum and Solar Minimum, NASA STI/Recon Technical Report N 77 (1976), p. 18983.
[34] G. Reitz, R. Beaujean, E. Benton, S. Burmeister, T. Dachev, S. Deme, M. Luszik-Bhadra, P. Olko, Space radiation measurements on-board iss—the DOSmap experiment, Radiat. Prot. Dosim. 116 (1–4) (2005) 374–379, https://doi.org/10.1093/rpd/nci262 http://rpd.oxfordjournals.org/content/116/1-4/374.abstract.
[35] T. Ersmark, P. Carlson, E. Daly, C. Fuglesang, I. Gudowska, B. Lund-Jensen, R. Nartallo, P. Nieminen, M. Pearce, G. Santin, N. Sobolevsky, Status of the desire project: geant4 physics validation studies and first results from columbus/iss radiation simulations, Nuclear Science Symposium Conference Record, vol. 3, IEEE, 2003, pp. 1540–1544, , https://doi.org/10.1109/NSSMIC.2003.1352170 3.
[36] R. Nymmik, Initial conditions for radiation analysis: models of galactic cosmic rays and solar particle events, Adv. Space Res. 38 (6) (2006) 1182–1190 https://doi.org/10.1016/j.asr.2006.07.002 http://www.sciencedirect.com/science/article/pii/S0273117706004315.
[37] M. Kruglanski, N. Messios, E.D. Donder, E. Gamby, S. Calders, L. Hetey, H. Evans, E. Daly, Last upgrades and development of the space environment information system (spenvis), European Conference on Radiation and its Effects on Components and Systems, 2009, pp. 563–565, , https://doi.org/10.1109/RADECS.2009.5994715.
[38] Space Environment (Natural and Artificial) — Galactic Cosmic Ray Model, Standard 15390, International Organization for Standardization, Geneva, CH, 2004.
[39] M.A. Chavy-Macdonald, A. Menicucci, G. Santin, H. Evans, P.T.A. Jiggens, P. Nieminen, S. Hovland, High-accuracy simulations of the iss radiation environment and applications to interplanetary manned missions, IEEE Trans. Nucl. Sci. 60 (4) (2013) 2427–2434, https://doi.org/10.1109/TNS.2013.2273375 http://ieeexplore.ieee.org/ielx7/23/6579700/06576916.pdf?tp=&arnumber=6576916&isnumber=6579700.
[40] Spacecraft Systems Branch, Flight Crew Support Division, National Aeronautics and Space Administration, Apollo Operations Handbook: Command and Service Modules vol. 2, National Aeronautics and Space Administration, 1968, http://books.google.com/books?id=IdgAHQAACAAJ.
[41] R.A. Braeunig, Orbital mechanics, [cited 2019], 2013. http://www.braeunig.us/space/orbmech.htm.
[42] Mission Planning And Analysis Division, Postflight Evaluation of the Apollo 14 Spacecraft Trajectories, Government Document MSC-04330, Manned Spacecraft Center, National Aeronautics and Space Administration, Houston, Tx, 1971.
[43] S.P. Hughes, R.H. Qureshi, D.S. Cooley, J.J. Parker, T.G. Grubb, Verification and Validation of the General Mission Analysis Tool (Gmat), (2014).
[44] C.E. Jordan, Nasa Radiation Belt Models Ap-8 and Ae-8, Report, DTIC Document, 1989.
[45] A.M. Marenny, R.A. Nymmik, E.D. Tolstaya, E.V. Benton, The radiation environment in near-earth space as treated in terms of different model representations,

Radiat. Meas. 26 (3) (1996) 493–496 https://doi.org/10.1016/1350-4487(96)00063-7 http://www.sciencedirect.com/science/article/pii/1350448796000637.
[46] R.S. Johnston, L.F. Dietlein, C.A. Berry, J.F. Parker, V. West, Biomedical Results of Apollo, Book NASA-SP-368, LC-75-600030, National Aeronautics and Space Administration, Washington, D.C., 1975.
[47] M.A. Xapsos, G.P. Summers, J.L. Barth, E.G. Stassinopoulos, E.A. Burke, Probability model for worst case solar proton event fluences, IEEE Trans. Nucl. Sci. 46 (6) (1999) 1481–1485, https://doi.org/10.1109/23.819111.
[48] J. Apostolakis, G. Folger, V. Grichine, A. Howard, V. Ivanchenko, M. Kosov, A. Ribon, V. Uzhinsky, D.H. Wright, Geant4 physics lists for hep, Nuclear Science Symposium Conference Record, 2008, NSS '08. IEEE, 2008, pp. 833–836, , https://doi.org/10.1109/NSSMIC.2008.4774655.
[49] Thomas Berger, Sönke Burmeister, Daniel Matthiä, Bartos Przybyla, Günther Reitz, Pawel Bilski, Michael Hajek, Lembit Sihver, Julianna Szabo, Iva Ambrozova, Filip Vanhavere, Ramona Gaza, Edward Semones, Eduardo G. Yukihara, Eric R. Benton, Yukio Uchihori, Satoshi Kodaira, Hisashi Kitamura, Matthias Boehme, Dosis & dosis 3d: radiation measurements with the dostel instruments onboard the columbus laboratory of the iss in the years 2009-2016, J. Space Weather Space Clim. 7 (2017) A8 https://doi.org/10.1051/swsc/2017005.
[50] C. Hill, Dose Assessment with Passive Detectors inside the Columbus Laboratory Onboard the International Space Station (iss), Thesis, (2010).
[51] E. Semones, Iss tepc Experiment Data, NASA Space Radiation Analysis Group, Johnson Space Center, National Aeronautics and Space Administration, 2001.